Synthesis and Tau RNA binding evaluation of ametantrone-containing ligands

Gerard Artigas, and Vicente Marchán*

Departament de Química Orgànica and IBUB, Universitat de Barcelona

Martí i Franquès 1-11, E-08028 Barcelona (Spain)

Fax: + (34) 93 339 7878

E-mail: vmarchan@ub.edu

SUPPORTING INFORMATION

Table of contents

1. Evaluation of the interaction between RNA and ligands.

1.1. UV-monitored melting experiments.

The solutions were 1 µM both in RNA (wt, +3, +14 or +16) and in ligands, in 10 mM sodium phosphate buffer pH 6.8, 100 mM NaCl and 0.1 mM Na_2EDTA. The samples were cooled from 90 ºC to 20 ºC at a constant rate of 0.5 ºC min^{-1} and the absorbance at 260 nm was measured as a function of temperature. The denaturation curves (20 ºC to 90 ºC) were also recorded. All experiments were repeated at least three times until coincident T_m values were obtained. The estimated error in T_m values was ± 0.2 ºC.

1.2. Fluorescence titration experiments.

First, the fluorescence emission spectra of the free ligand in the previous buffer were recorded. Subsequent aliquots of a wt RNA solution in the same buffer (previously folded by heating the solution for 5 min to 90 ºC and left to slowly cool to RT) were added to the ligand's solution, and the fluorescence emission spectra were recorded.

1.3.Fluorescence binding assays.

Fluorescence measurements were performed in 1-cm path-length quartz cells on a QuantaMaster fluorometer (PTI) at 25 ºC, with an excitation slit width of 4.8 nm and an emission slit width of 8 nm. Upon excitation at 490 nm, the emission spectrum was recorded over a range between 505 and 540 nm until no changes in the fluorescence intensity were detected. All binding assays were performed in the melting curves' buffer. The sample was continuously stirred except during the fluorescence measurement. First, the fluorescence spectrum of the buffer was recorded, to be used as the baseline. For each experiment, the spectrum of a 25 nM solution of refolded fluorescein-derivatized RNA (25 pmol in 1 mL buffer) was recorded, and the baseline blank subtracted. Subsequent aliquots of 1 µL of aqueous ligand' solutions (of increasing concentrations, depending on the ligand's affinity) were added to the RNA-containing solution.

The fluorescence spectrum was recorded after addition of each aliquot until the fluorescein fluorescence signal at 517 nm reached saturation (typically 5–10 min). Over the entire range of ligand concentrations used, the emission maxima varied less than 1 nm. The total volume of the sample never changed more than 10-15 %. The full titration was repeated in the absence of labelled RNA to correct for the presence of the ligand's fluorescence. These spectra were subtracted from each corresponding point of the labelled RNA titrations, and the resulting fluorescence intensity was corrected for dilution ($F'=F_{*}V/V_0$).

The emission fluorescence at 517 nm was normalized by dividing the difference between the observed fluorescence, *F'*, and the final fluorescence, F_f, by the difference between the initial fluorescence, F_0, and the final fluorescence, F_f. This normalized fluorescence intensity was plotted as a function of the logarithm of the total ligand concentration in each point of the titration. Finally, nonlinear regression using a sigmoidal dose-response curve was performed with the software package GraphPad Prism 4 (GraphPad Software, San Diego, CA) to calculate the EC_{50} values. Experimental errors were less than or equal to ± 25% of each value.

For competitive experiments, a tRNA from baker's yeast (*S. cerevisiae*) was purchased from Sigma. Stock solutions of $tRNA^{mix}$ were quantified using an average extinction coefficient of 9.640 cm^{-1} per base. The fluorescence binding assays were carried out as described above with the exception that a 30-fold excess (base) of the $tRNA^{mix}$ was added to the refolded fluorescein-labelled RNA (or to the buffer for the titration without target RNA).

1.4. NMR Spectroscopy.

NMR spectra were acquired in a Bruker Advance spectrometer operating at 600 MHz, and processed with Topspin software. Samples were dissolved in 10 mM phosphate buffer, pH 6.8, in H_2O/D_2O 9:1.

For titration experiments, wt RNA (60 nmol) was dissolved in 600 µL of 10 mM sodium phosphate buffer (pH 6.8), and 2 µL of a 33.3 µM solution of DSS in water were added. After lyophilization, the residue was dissolved in 600 µL of a 9:1 H_2O/D_2O mixture. Annealing was performed by heating at 90ºC for 3 min, followed by snap cooling on ice for 20 min. NMR spectra were recorded at 5ºC to minimize the exchange with water. Water suppression was achieved by using an excitation sculpting sequence (zgesgp). Subsequent 1D ^1H NMR spectra were recorded at 5ºC upon addition of increasing quantities of ligand (0.5, 1.0, 1.5 and 2.0 mol equiv.). The total volume of the sample never changed more than 5%.

2. Reversed-phase HPLC analysis of the ligands

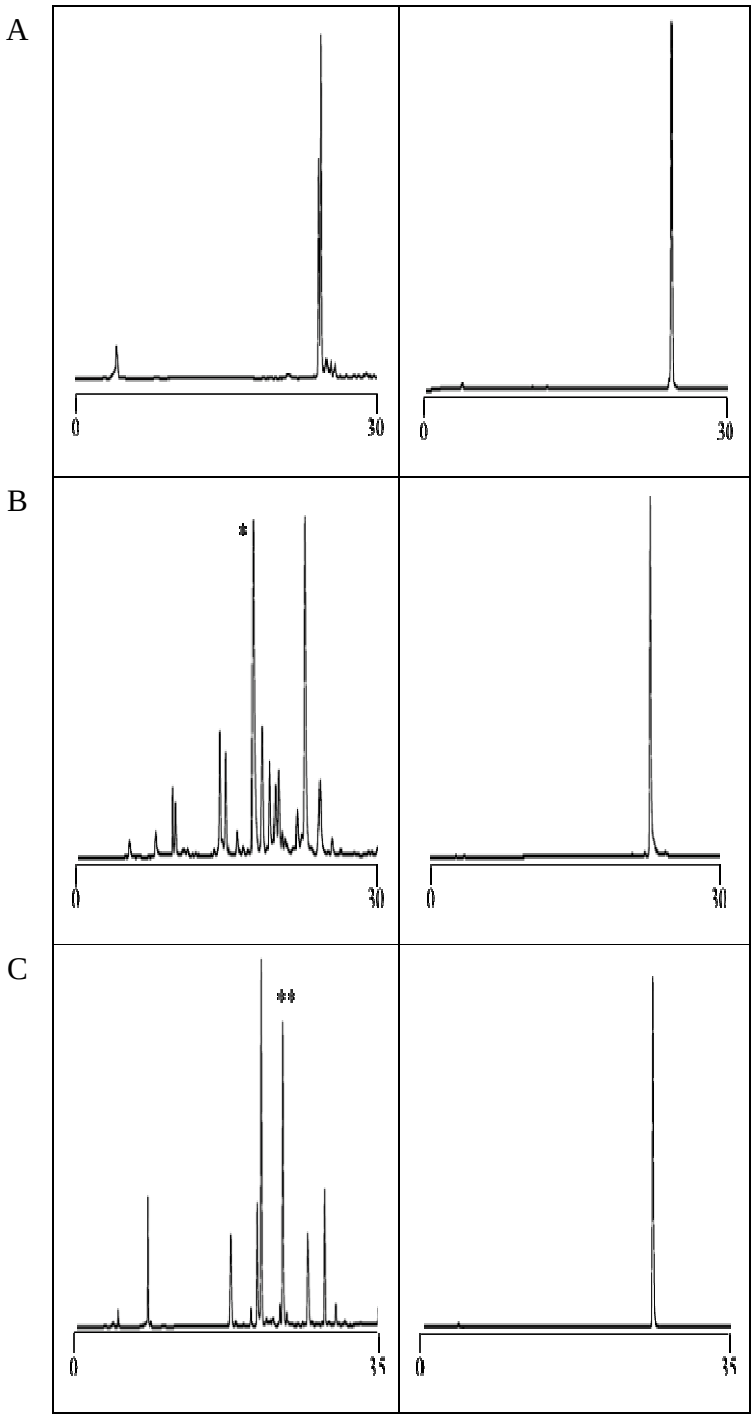

Figure S1 Reversed-phase HPLC traces for the ligands Amt-NeaG4 (A), Amt-Nea,Nea (B) and Amt-Nea,Azq (C): reaction crude (left) and purified (right).

3. ^{1}H NMR spectra of the ligands

Amt-NeaG4

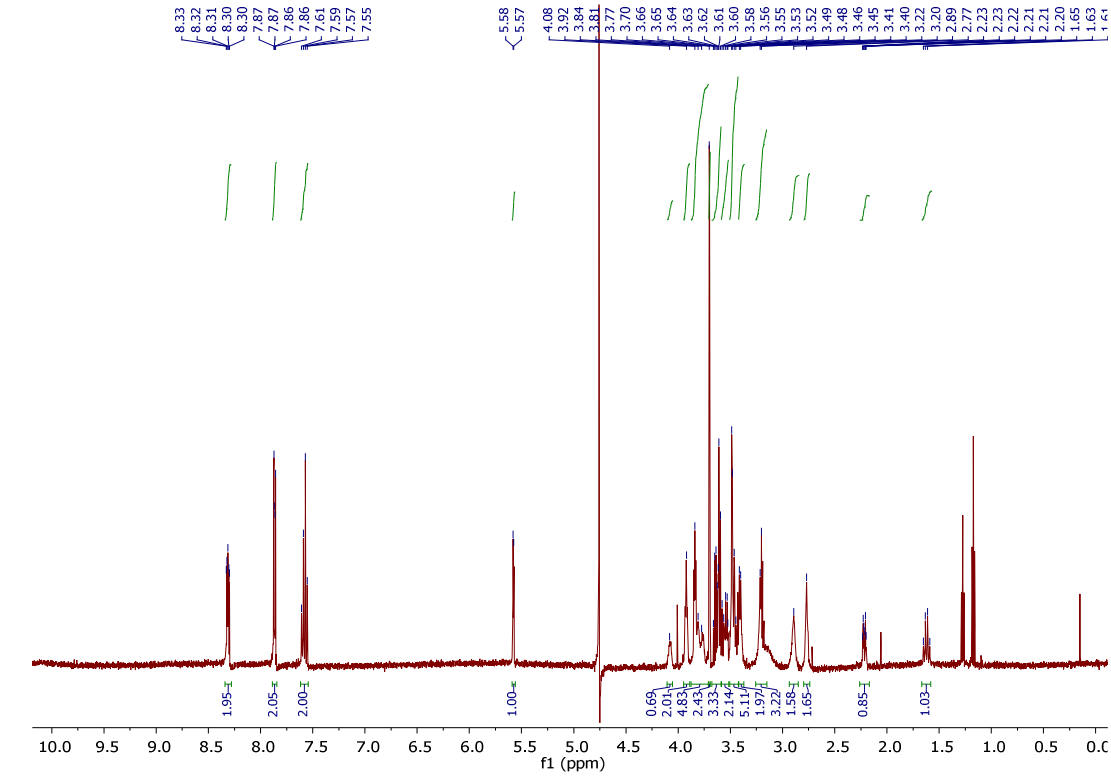

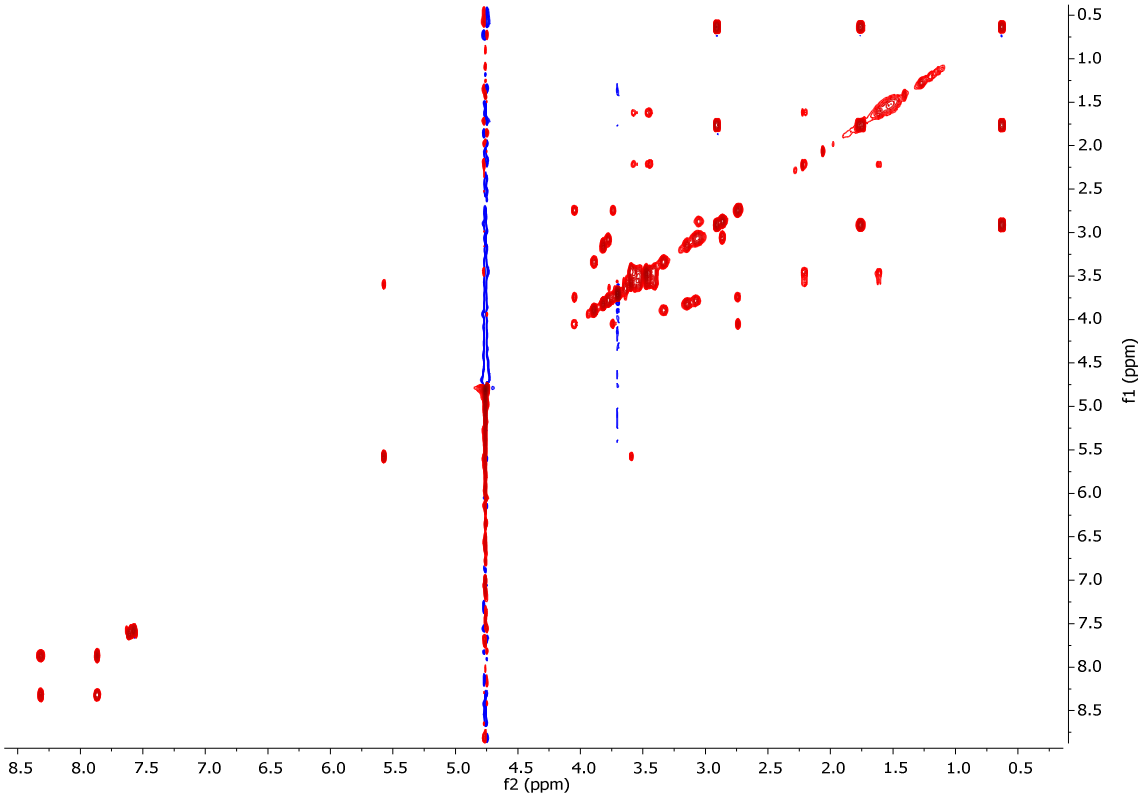

Amt-Nea,Nea

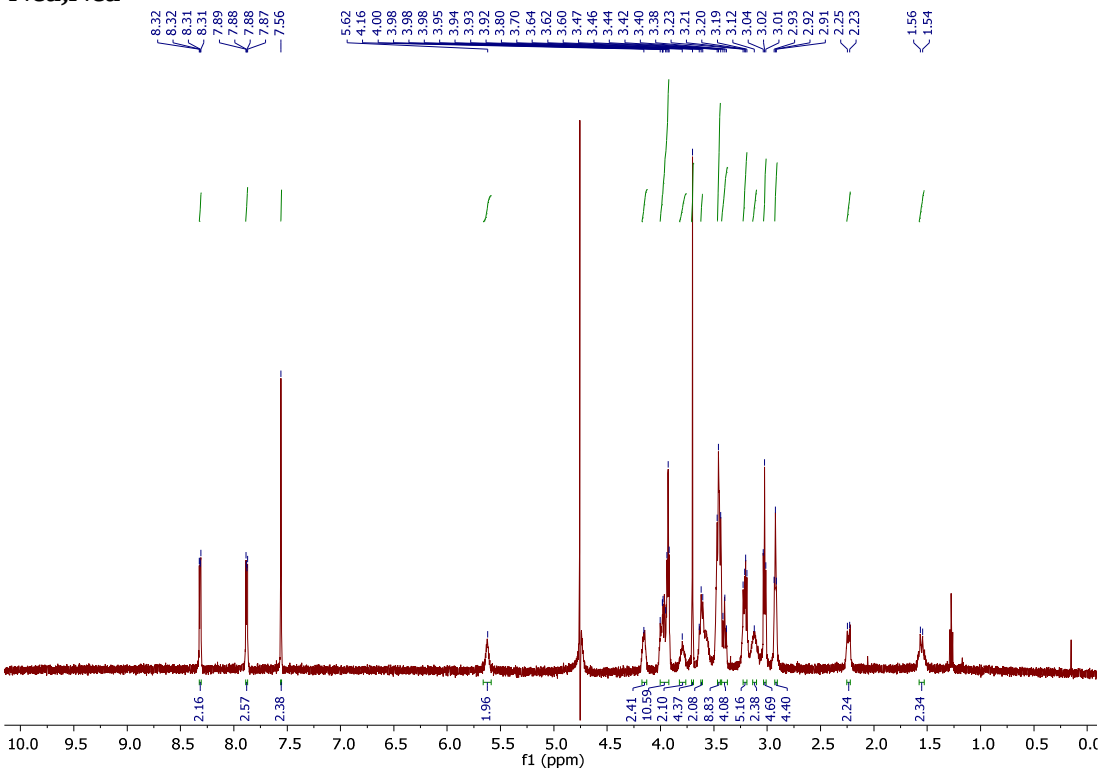
8.32
8.32
8.31
8.31
7.89
7.88
7.88
7.87
7.56
5.62
4.16
4.00
3.98
3.98
3.98
3.95
3.94
3.93
3.92
3.80
3.70
3.64
3.62
3.60
3.47
3.46
3.44
3.42
3.40
3.38
3.23
3.21
3.20
3.19
3.12
3.04
3.02
3.01
2.93
2.92
2.91
2.25
2.23
1.56
1.54
2.16
2.57
2.38
1.96
2.41
10.59
2.10
4.37
2.08
8.83
4.08
5.16
2.38
4.69
4.40
2.24
2.34
f1 (ppm)

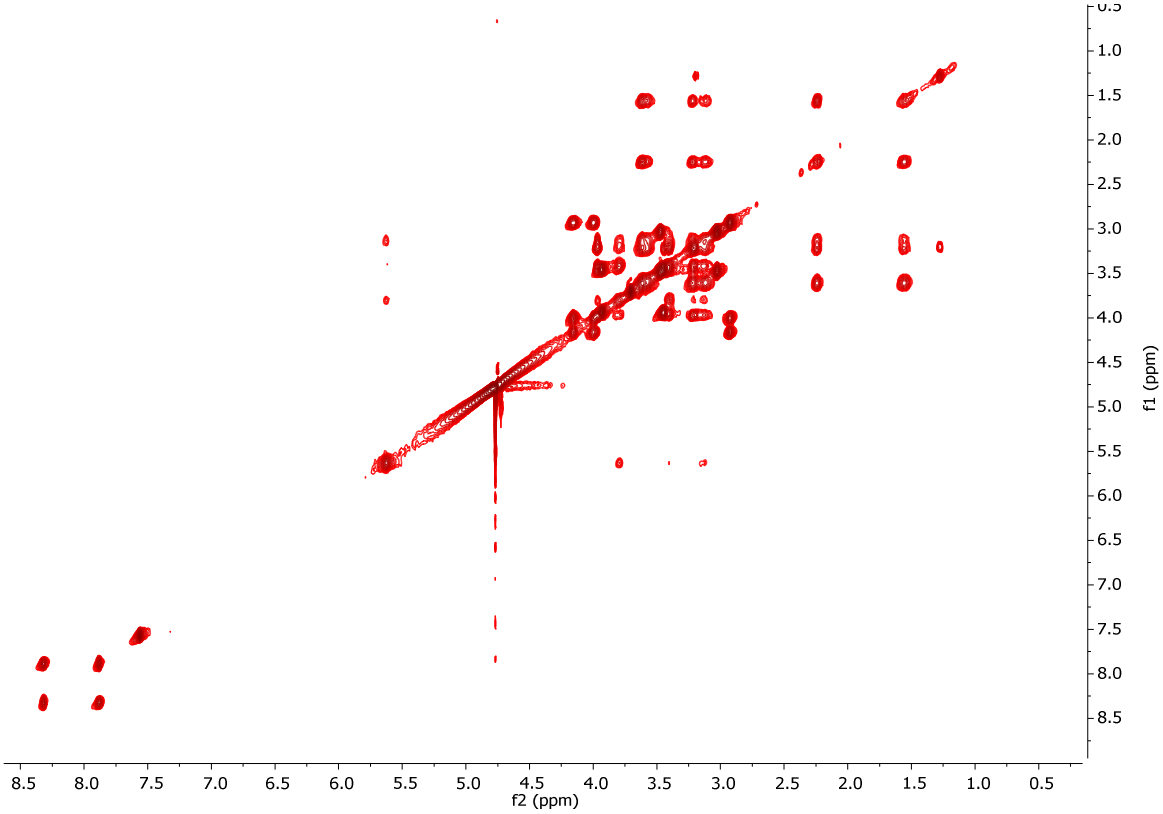
f2 (ppm)
f1 (ppm)

Amt-Nea,Azq

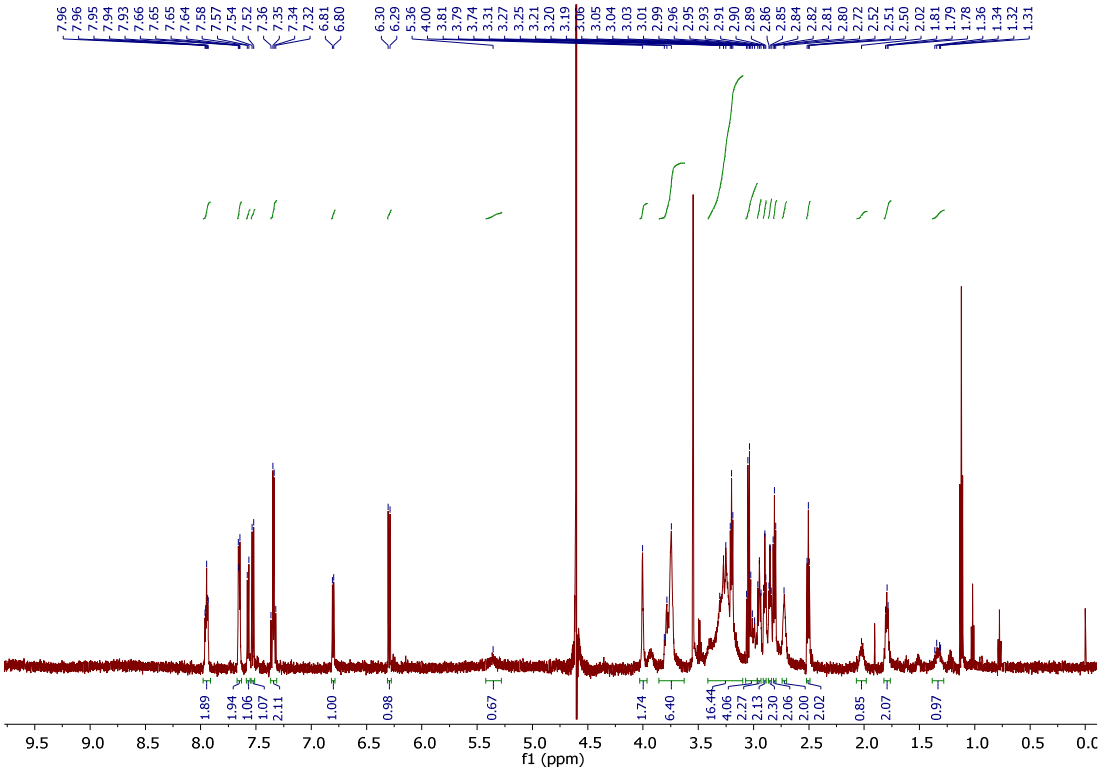
7.96 7.96 7.95 7.94 7.93 7.66 7.65 7.65 7.64 7.58 7.57 7.54 7.52 7.36 7.35 7.34 7.32 6.81 6.80
6.30 6.29 5.36 4.00 3.81 3.79 3.74 3.31 3.27 3.25 3.21 3.20 3.19 3.06 3.05 3.04 3.03 3.01 2.99 2.96 2.95 2.93 2.91 2.90 2.89 2.86 2.85 2.84 2.82 2.81 2.80 2.72 2.52 2.51 2.50 2.02 1.81 1.79 1.78 1.36 1.34 1.32 1.31
1.89 1.94 1.06 1.07 2.11 1.00 0.98 0.67 1.74 6.40 16.44 4.06 2.27 2.13 2.30 2.06 2.00 2.02 0.85 2.07 0.97
f1 (ppm)

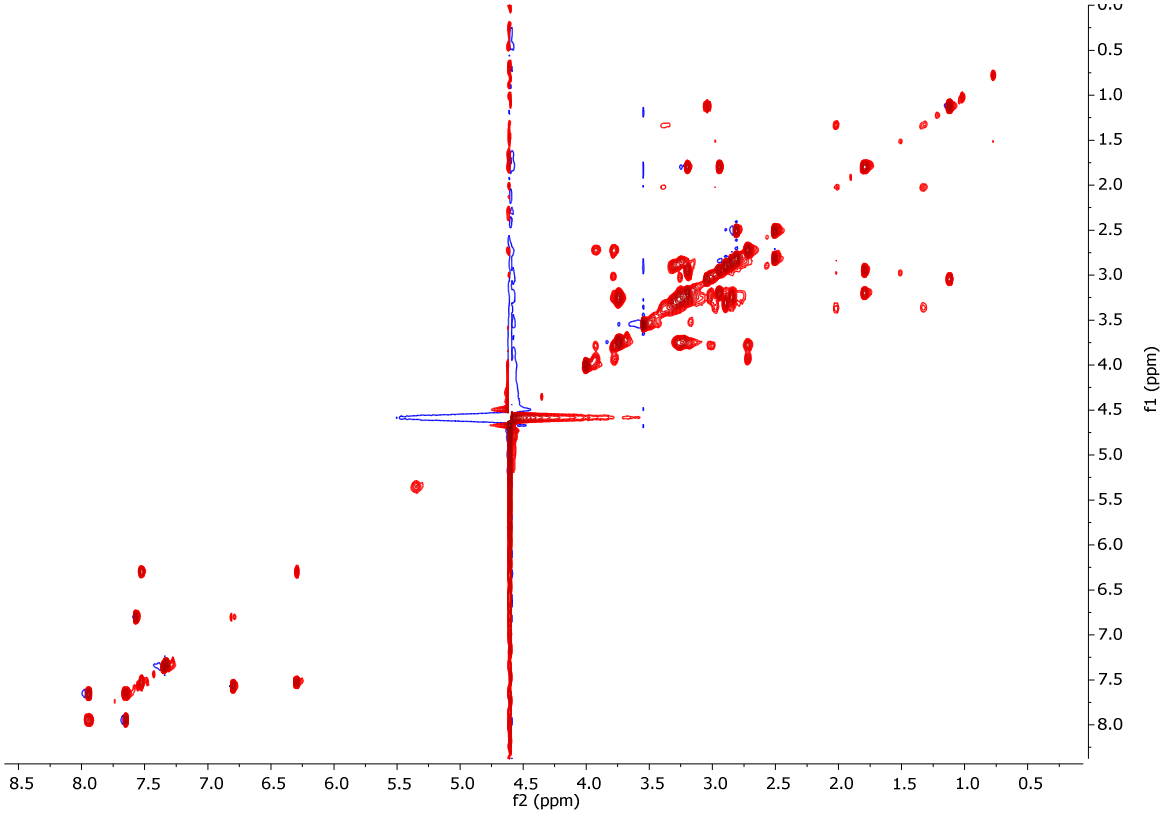
f2 (ppm)
f1 (ppm)

4. UV melting curves of RNA-ligand complexes

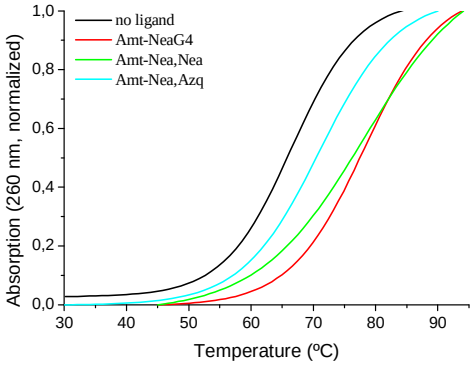

Figure S2. UV melting profiles for the wt RNA oligonucleotide and its ligand complexes at a [ligand]/RNA ratio of 1.0.

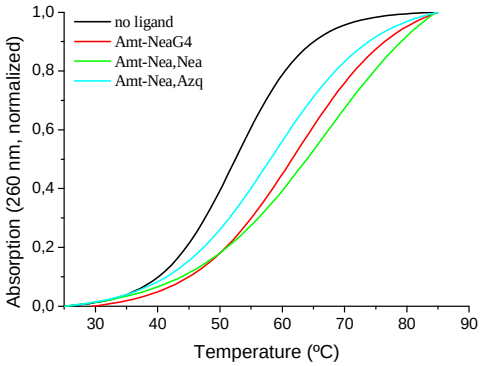

Figure S3. UV melting profiles for the +3 mutated RNA oligonucleotide and its ligand complexes at a [ligand]/RNA ratio of 1.0.

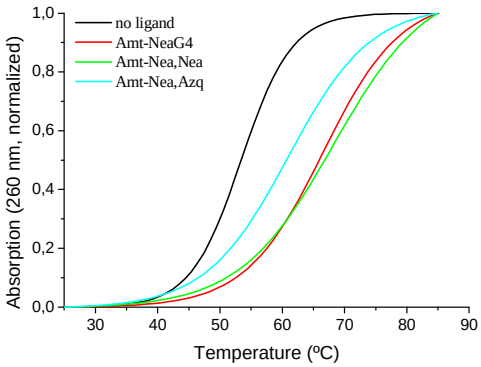

Figure S4. UV melting profiles for the +14 mutated RNA oligonucleotide and its ligand complexes at a [ligand]/RNA ratio of 1.0.

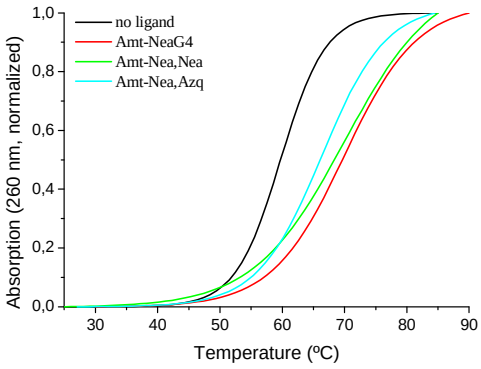

Figure S5. UV melting profiles for the +16 mutated RNA oligonucleotide and its ligand complexes at a [ligand]/RNA ratio of 1.0.